UNITED STATES DEPARTMENT OF THE INTERIOR

GEOLOGICAL SURVEY

GARNET PERIDOTITES FROM WILLIAMS KIMBERLITES, NORTH-CENTRAL MONTANA, USA

by

B. C. Hearn, Jr., and E. S. McGee

U.S. Geological Survey
OPEN-FILE REPORT 83-172

1983

CONTENTS

TABLES

ILLUSTRATIONS

GARNET PERIDOTITES FROM WILLIAMS KIMBERLITES,
NORTH-CENTRAL MONTANA, USA

---

by B. C. Hearn, Jr., and E. S. McGee

Abstract

Two Williams kimberlites, 250x350m and 37x390m, in the eastern part of a swarm of 30 middle Eocene alnoitic diatremes in north-central Montana, USA, contain xenoliths of garnet-bearing lherzolites, harzburgites and dunites, in addition to spinel peridotites and upper and lower crustal amphibolites and granulites. Colluvial purple, red, and pink garnets are dominantly Mg- and Cr-rich, indicating their derivation from peridotites or megacrysts, and have CaO and Cr_2O_3 contents that fall in the lherzolite trend.

Temperatures were calculated by the Lindsley-Dixon 20 kb method for lherzolites and by the O'Neill-Wood method for harzburgites and dunites, and pressures were calculated by the MacGregor method, or were assumed to be 50 kb for dunites. Most peridotites equilibrated at 1220-1350°C and 50-60 kb, well above a $44mW/m^2$ shield geotherm and on or at higher P than the graphite-diamond boundary. Four lherzolites are low T-P (830-990°C, 23-42 kb) and are close to the shield geotherm. All four low T-P lherzolites have coarse textures whereas the high T-P cluster has both coarse and porphyroclastic textures, indicating a range of conditions of deformation and recrystallization in a restricted high T-P range. The tiny size (0.01-0.2 mm) of granulated and euhedral olivines in several xenoliths shows that deformation was occurring just prior to incorporation in kimberlite and that ascent was rapid enough (40-70 km/hr) to retard further coarsening of fine-grained olivine. For other high T-P peridotites, cessation of deformation and beginning of recrystallization before or during inclusion in kimberlite is suggested by larger (up to 3mm) euhedral olivines in a matrix of fine granulated olivine or by optical continuity of large and nearby small olivines.

Two low T-P lherzolites contain distinctive, phlogopite-rimmed, 5-8mm clots of moderate-Cr garnet + Cr-spinel + Cr-diopside ± enstatite that are inferred to have formed by reaction of an initial high-Cr garnet brought into the garnet + spinel stability field. This suggests a reduction in pressure and temperature prior to inclusion in the kimberlite, followed by metasomatic introduction of phlogopite. These textural and compositional variations of peridotites seem most compatible with kimberlite generation and ascent during dynamic diapiric perturbation of the upper mantle.

Geology of the Williams Diatremes

The Williams kimberlites are a group of four closely spaced diatremes (fig.1) in the eastern part of an east-northeast trending swarm of 30 ultramafic alkalic diatremes, dikes, and plugs (Hearn, 1968, 1979) having ages of 46 to 51 m.y. (middle Eocene) (Marvin and others, 1980) in the Missouri River Breaks area of north-central Montana. The ultramafic alkalic diatremes are the youngest igneous episode in a 25 m.y. span of alkalic igneous activity east of the northern Rocky Mountains in Montana (Marvin and others, 1980). The western end of the swarm is represented by the Haystack Butte intrusion (Buie, 1941) on the eastern flank of the Highwood Mountains, and the easternmost occurrence is the Ricker Butte group of intrusions, on the southeast flank of the Little Rocky Mountains. The diatremes and intrusions were produced by alkalic ultramafic magmas that crystallized to alnoite or monticellite peridotite within and outside of the diatremes. Their fine-grained chilled products in bedded pyroclastic deposits within the diatremes, if fresh, would correspond to olivine nephelinite or olivine melilitite, but are typically altered to secondary assemblages. Such alkalic ultramafic magmas occur in the same broad geographic areas as kimberlites in other parts of the world (Dawson, 1980), and are likely to have been parental to many kimberlites. Although the alkalic ultramafic character of the Missouri Breaks diatremes indicates kimberlitic affinity, only the Williams diatremes can be termed true kimberlite on the basis of the presence of the typical kimberlite indicator minerals chromian pyrope, chromian diopside, enstatite, and magnesian ilmenite (Dawson, 1980). No diamonds have been reported from the Williams kimberlites.

The Precambrian basement consists of Archaean schists, gneisses and amphibolites (2550 m.y. or older) that have been overprinted by early Proterozoic metamorphism (1710-1750 m.y.) (Peterman, 1981). Precambrian rocks are exposed 7 to 20 km to the northeast in the Little Rocky Mountains uplift. The crust is 50 km thick in northern Montana (McCamy and Meyer, 1964).

Two of the Williams diatremes are major pipes and two are smaller, satellitic pipes. Williams 1 is very poorly exposed and was mapped by soil types, presence of indicator minerals in soils and in animal burrows, and limited soil-auger sampling. After completion of the mapping, artificial exposures were available in about 25 trenches dug during commercial exploration during 1980 and 1981. Williams 1 is a diatreme of rounded triangular shape, about 250 by 350 m in size, which has been emplaced against the ring fracture of the core of the Siparyann Butte (Thornhill Butte) dome, a dome of Cretaceous to Cambrian sedimentary rocks that were uplifted about 61 m.y. ago above a hornblende syenite porphyry intrusion (Brockunier, 1936; Knechtel, 1959; Marvin and others, 1980). Wall rock of the west, south and north sides of the kimberlite is dominantly shale, with minor beds of limestone and sandstone, of the Colorado Group of Cretaceous age. Wall rock to the east is Paleozoic limestone, dolomite, and calcareous shale in the dome. The diatreme mainly contains soft, clay-rich kimberlite breccia, which is rich in inclusions of Cretaceous and early Eocene sedimentary rocks, and shows poorly defined bedding in only one of about 25 trench exposures. This lack of bedding is in strong contrast to diatremes elsewhere in the swarm that contain bedded fragmental deposits as much as 1500 m below the surface of eruption. A small intrusion of massive kimberlite or partially altered monticellite peridotite is present in the southern part. Downfaulted blocks of sandstone and claystone of the Wasatch Formation (early Eocene), about five to a few tens of meters in size, occur on the border of the Williams 1 diatreme. Other Missouri Breaks diatremes contain similar large slices of sedimentary rocks (from the Wasatch and older formations) that have subsided as much as 1500 m. Blocks of Cretaceous shale and sandstone, from one to several meters in size, are also present.

The presence (in panned concentrates), of olive-green pyroxenes of slightly rounded, prismatic euhedral shape, and presence of rare pebbles of phonolite, indicate that the diatreme also incorporated detrital material derived from the Bearpaw Mountains volcanic field of middle Eocene age (54-50 m.y.) (Hearn, 1979; Marvin and others, 1980) 40 km to the northwest.

The poorly exposed Williams 2 pipe, about 40 by 120 m, contains kimberlite breccia amidst large amounts of limestone and dolomite fragments from the surrounding Paleozoic rocks. Williams 3, about 30 by 40 m, primarily consists of one or more blocks of sandstone and siltstone that have subsided a few hundred meters from the Eagle Sandstone or from the Telegraph Creek Formation, and occupy the whole pipe area except for a small marginal occurrence of kimberlite breccia.

Williams 4 is a dike-like diatreme, 390 m long and up to about 40 m wide. Parts of Williams 4 are well exposed. The dike is variable in texture along strike. Massive kimberlite forms several areas from two to a few tens of meters across; the rest of the dike has fragmental texture or is unexposed. Some massive outcrops show cryptic fragmental texture. A portion of the dike near its southwestern end contains abundant autoliths 0.5 to 8 cm in diameter. Most autoliths contain cores of baked shale, baked sandstone, or igneous rock (kimberlite or monticellite peridotite?) of slightly coarser texture than the peripheral micaceous igneous coating. A very few autoliths contain cores of garnet megacrysts or altered peridotite.

Potassium-argon dating of two sizes of phlogopite (+28 mesh and 100 to 150 mesh) yielded ages of 399± 14 m.y. and 166± 6 m.y. respectively, too old to fit the geological age. Coarse-grained phlogopite from a vein in the intrusion in the southern part of Williams 1 diatreme gave an age of 47.5 ± 1.6 m.y., in accord with presence of inclusions of early Eocene sedimentary rocks and of clasts of middle Eocene volcanic rocks (Marvin and others, 1980).

The mapped limits of the Williams 1 diatreme were verified or slightly modified by later magnetic mapping (fig. 2). The magnetic survey was done by B. C. Hearn, Jr. using a Geometrics model G-816/826 proton magnetometer. On September 8, 1979, magnetic readings were taken at 50 feet (15 m) spacing, and locally at 25 feet (7.5 m) spacing, along five lines. The station locations were determined by pacing distance along the lines and by reference to prominent features on an enlarged aerial photograph at 1:2640 scale (1 inch = 220 feet). Between July 26 and August 1, 1980, a more complete survey was done by measuring magnetic values at marked stations on a 50 feet (15 m) grid, with subsidiary stations at 25 feet (7.5 m) spacing where more detail was needed. The grid was established by tape and Brunton compass. Linear corrections for diurnal variation were calculated from readings at a base station every 1 to 1.5 hours. Magnetic values are probably accurate to ± 2 gammas.

The diatreme is expressed as a rather flat-topped positive anomaly of 60 gammas that has steep gradients of 40-60 gammas within 30 meters or less across the border and has a superimposed 600 gamma anomaly over the massive intrusion in the southern part. The magnetic gradient is on the inner edge of the large descended inclusions (which are non-magnetic) on the northwest, north and east margins of the diatreme. The disparity between the geologically and magnetically mapped contacts in the southeast part may be due to westward slumping of wall rock. Williams 2 diatreme shows magnetically as a 60 m circular positive anomaly of 300 gammas that approximately corresponds to only two-thirds of the mapped limits of the pipe, probably as a result of extreme dilution of part of the kimberlite by abundant inclusions. The Williams 3 diatreme lacks magnetic expression because the kimberlite is too small near the surface, or is too diluted by inclusions or is too deep. The Williams 4 dike has positive anomalies of 300 to 400 gammas in three traverses across the southern half.

Inclusions from deep levels -Inclusions which have ascended in the Williams kimberlites are from the shallow Precambrian basement (below 2000 m) and deeper parts of the upper crust (schist, gneiss, amphibolite), from the lower crust (granulite, mafic granulite, mafic amphibolite), and from the upper mantle (spinel peridotite, spinel pyroxenite, dunite, garnet peridotite, garnet pyroxenite, garnet megacrysts, xenocrysts of kimberlite indicator minerals). No eclogites have been found. Assignment of lithologies to the upper or lower crust is tentative and based on analogies with inclusion suites in diatremes in other regions, and on textures and facies of sequences of metamorphic rocks in other regions. Garnets occur in rocks from each of the above listed depth zones. Study of the entire suite of inclusions is in progress, but thus far has been concentrated on the upper-mantle garnet peridotites.

Garnet peridotites and pyroxenites -- The suite of six garnet peridotites previously reported (Hearn and Boyd, 1975) has been augmented by recent collections, for a total of about 100 peridotite nodules from the surface and from shallow exploration trenches in the Williams 1 and 4 diatremes. Peridotite nodules typically have an outer rind of alteration comprising 25 to 100 percent of their volume, leaving only garnet and diopside, and in some nodules, only garnet, surviving from the original assemblages. The sizes of nodules range from 1 to 30 cm, and are dominantly 2 to 5 cm.

Relative abundance of peridotite-pyroxenite mineral assemblages is shown in Table 1. The term lherzolite is used for olivine-two pyroxene assemblages, including those that contain as little as 0.1 percent clinopyroxene, and generally conforms to the usage of the term by others in studies of ultramafic nodules (Dawson, 1980). The nodule suite is dominated by garnet-bearing assemblages (64 of 100): 51 garnet lherzolites, 7 garnet harzburgites, 3 garnet pyroxenites, and 2 garnet dunites. Of these, 14 contain both garnet and spinel, typically with 0.1 - 0.5mm spinel and clinopyroxene grains either surrounding 2-5 mm garnets, or less commonly, dispersed in garnet.

Textures of garnet peridotite inclusions

Individual peridotite inclusions have rather uniform textures, either sheared (porphyroclastic and mosaic porphyroclastic textures of Harte, 1977) (fig. 3) indicating varying degrees of deformation; or granular, unsheared (coarse-equant and coarse-tabular textures of Harte, 1977) (fig. 4) indicating textural equilibration. The suite as a whole shows a complete range from undeformed coarse textures to intensely deformed mosaic porphyroclastic textures. The range of textures may represent part of a cyclic progression of textural development (Harte, 1975). Minerals typically show increasing resistance to deformation in the order: olivine, clinopyroxene, orthopyroxene, garnet. Good examples of the more intense deformation textures (such as the disrupted, laminated, and fluidal subgroups of porphyroclastic textures in the classification of Harte (1977)) have not been found. Some inclusions do, however, show crude layering of porphyroclasts and fine-grained olivine and are thus approaching laminated texture. Also, one small harzburgite (H67-28K-3, fig. 1B, Hearn and Boyd, 1975) has disrupted texture of garnet. Granoblastic textures (grain size less than 2 mm, straight or smoothly curving grain boundaries, Harte, 1977) have not been found.

Mosaic porphyroclastic inclusions contain three generations of olivine: highly strained porphyroclasts (maximum size up to 2 cm) that are survivors of the pre-deformation coarser texture, fine-grained anhedral olivine neoblasts that are known or assumed to be recrystallized and strain-free, and strain-free euhedral olivine neoblasts as much as 3 mm size that represent the latest growth of olivine.

Euhedral neoblasts show preferred orientation in some peridotites. Strain-free euhedral neoblasts clearly grew after deformation had ceased (after granulation of olivine). The post-deformational timing of growth is especially evident for euhedral neoblasts that extend across bands of fine-grained anhedral olivine. Growth of euhedral neoblasts could have occurred either just before incorporation or within the kimberlite fluid in the short period of time between incorporation of inclusions and near-surface emplacement of the kimberlite.

Experimental data on deformation of natural dunites at 10 kb show that grain size of anhedral olivine neoblasts during steady-state deformation is inversely related to stress and is independent of temperature under dry or damp (0.3 percent water) conditions, whereas under wet conditions, grain size of anhedral neoblasts is directly proportional to temperature as well as inversely proportional to stress (Ross and others, 1980). The small size of the fine-grained olivines in porphyroclastic inclusions implies that deformation of peridotite was occurring within a few hours before incorporation in the kimberlite, as longer times would have allowed olivine to coarsen (Mercier, 1979). In experimental runs, euhedral neoblasts do not form during steady-state deformation or under wet conditions. Euhedral neoblasts form under dry or damp, static conditions during "primary annealing recrystallization" (Mercier, 1979), and grow at the expense of strained porphyroclastic olivines, with a growth rate dependent upon the stored strain energy (related to the previous differential stress) and on the temperature (Mercier, 1979, fig. 4A). Presence of euhedral olivine neoblasts in peridotite inclusions implies dry conditions during recrystallization, i.e. minimal influence of hydrous fluids (Mercier, 1979, p. 204).

The size of euhedral neoblasts can be used to calculate the average velocity of ascent of the kimberlite host (Mercier, 1979, p. 207). In a suite of inclusions derived from approximately the same depth, those with smaller neoblasts imply faster rates of ascent. Variation of calculated velocities within the same pipe could suggest that some neoblast growth occurred in the wall rock or in the kimberlite before rapid ascent. The fastest rate of inclusion ascent is the most likely rate of ascent of the kimberlite. An intensely deformed Williams inclusion (H69-15F) has euhedral and anhedral neoblasts of sizes similar to those in sample PHN-1596 (Mercier, 1979, table 1), and thus has similar calculated times of ascent, 3 to 5 hours (velocities 40 to 70 km/hr), for assumed initial temperatures of 1625 or 1725 degrees C respectively for the kimberlite host.

In addition to the development of euhedral neoblasts, the suite of sheared xenoliths shows other partial annealing textures. An unusual texture of optical continuity of a large strained olivine and about 10 to 20 isolated small anhedral olivine grains in the adjacent matrix of fine-grained olivines suggests that recrystallization into uniform orientation has occurred on a small scale without euhedral growth or major increase in grain size. Other inclusions show sub-linear arrays of medium-sized olivines that have nearly the same crystallographic orientation.

Several garnet-spinel peridotites show an unusual texture (figs. 4 and 5) of garnet-clinopyroxene-spinel clots, rimmed by phlogopite. The clots are 5-7 mm garnets that contain numerous 0.05-0.5 mm clinopyroxene and opaque spinel grains, and rare small orthopyroxene grains. Phlogopite rims are 1-2 mm wide, consist of 0.2-1 mm phlogopites, and contain scattered 0.1-0.3 mm clinopyroxene grains, 0.05-0.2 mm opaque spinels, and in the inner half, contain fine-grained vermicular-textured brown translucent spinel. Some garnets also contain rounded, larger primary inclusions of olivine or clinopyroxene. A few larger (0.5-2 mm) spinels are not associated with garnet clots.

The abundant clinopyroxenes and Cr-rich spinels in garnet clots indicate a textural disequilibrium because the small grains have not enlarged and coalesced. We interpret this texture to be an interrupted reaction of Cr-rich garnet breaking down to a lower-Cr garnet + clinopyroxene + Cr-rich spinel ± rare orthopyroxene. It is not a reaction between olivine and garnet, as clinopyroxene and spinel are absent between garnet and included olivine (fig. 5). The timing of development of garnet-clot textures in low T-P xenoliths is not known, but may be related to alkalic magmatism from Paleocene to Middle Eocene time in the region. Clot textures are too coarse to attribute to a kelyphitization process, but appear too fine-grained to have persisted for tens of millions of years. The relatively shallow calculated depths of clot-bearing xenoliths preclude any direct relation between clot development and generation of the kimberlite. More detailed study of zoning profiles and kinetic effects may clarify the timing of partial re-equilibration. In a later reaction, rims of phlogopite grew at the expense of garnet on the periphery of garnet clots, engulfed opaque spinel and clinopyroxene of the clots, and produced fine-grained vermicular translucent brown spinel in the inner part of the phlogopite rim. Phlogopite in peridotite nodules is commonly considered to be a metasomatic component that was introduced in the upper mantle long before kimberlite ascent, or shortly before inclusion in the kimberlitic magma, or introduced during ascent. In an even later reaction, at shallow depth, outer edges of garnets and numerous small areas within garnets have been replaced by an incipient kelyphitic(?) alteration of unknown dusty brown material that contains abundant tiny anhedral to euhedral translucent brown Al-rich spinels.

Mineral compositions

Garnet

Garnets from 19 fresh and eleven altered ultramafic inclusions have been analysed (table 2, and Hearn and McGee, 1982; Hearn and Boyd, 1975). Garnets are pyrope-rich with Mg/(Mg + Fe) of 0.78 to 0.88 (figs. 6 and 8). Cr_2O_3 content exceeds 4.0 percent in 18 of the 19 fresh inclusions, and in 9 of 11 altered peridotites (fig. 7). All of the peridotitic garnets with more than 4.0 percent Cr_2O_3 are purple, the typical color of Cr-rich pyrope which aids in the field recognition of peridotitic garnets in prospecting for kimberlites (Leighton and McCallum, 1979; Dawson, 1980; Hearn and McGee, 1982). Peridotite garnets with less than 4.0 percent Cr_2O_3 are red or red-orange.

Garnets are typically unzoned or show a small range of composition within each xenolith, except in garnet-clinopyroxene-spinel clots (figs. 4 and 5) in low temperature (T)-low pressure (P) lherzolites, and in one dunite and one high T-P lherzolite. Garnets in clots have a range of 3.3 to 4.9 percent Cr_2O_3, indicative of incomplete re-equilibration during formation of Cr-spinel, clinopyroxene, and sparse orthopyroxene, and in keeping with the slower rates of equilibration of garnet compared to olivine and pyroxenes (Smith, 1982). Variable Cr_2O_3 values of garnet have no systematic relation to position in the clot, or to proximity of clinopyroxene, spinel, internal kelyphitic(?) alteration patches, or the border of the garnet clot (fig. 5). The reason for Cr_2O_3 variability in a single garnet in a dunite (T3-3, 9.4-11.6 percent) and between garnets in a lherzolite (H80-12E-2, 9.9-10.7 percent) is unknown; both have high T-P of equilibration, have garnets of high Cr_2O_3 content, and contain Cr-rich spinel in apparent equilibrium with garnet.

Garnets show a typical inverse relation of Cr and Al owing to the substitution in the six-coordinated position. Cr_2O_3 content is directly proportional to CaO content, even for garnets of variable composition within single inclusions (fig. 7). The Cr_2O_3-CaO variation is within or slightly more CaO-rich than the trend of lherzolite garnets (Sobolev and others, 1973). The lherzolitic Cr_2O_3-CaO relation holds for harzburgite and dunite garnets as well, which suggests that both equilibrated with clinopyroxene and orthopyroxene nearby, although one or both pyroxenes are absent. No peridotite inclusions contain garnets of low CaO and high Cr_2O_3 (group 10, low-calcium chrome-pyrope, Dawson and Stephens, 1975, 1976) that are favorable for the presence of diamond. Group 10 garnets are characteristic of some garnet inclusions in diamond and of a group of CaO-poor garnet harzburgites and garnet dunites that commonly contain Cr-rich spinel and rarely contain diamond (Gurney and Switzer, 1973; Boyd and Finnerty, 1980; Sobolev and others, 1973). Cr_2O_3 contents of garnets from peridotites suggest a bimodal distribution, with a gap between about 2 and 4 percent Cr_2O_3 in which only an orthopyroxenite garnet and the lower Cr_2O_3 portions of the range for clot garnets in lherzolites are represented. A similar bimodal distribution of Cr_2O_3 in garnets has been noted for kimberlites of Somerset Island, Canada by Mitchell (1979, p. 163) as a justification for subdividing the garnets of group 9 (chrome pyrope) of Dawson and Stephens (1975, 1976) into high and low Cr_2O_3 subgroups. The bimodal distribution may be present in sparse data shown by McCallum, Eggler and Burns (1975, p. 174) for garnets from peridotites in Colorado-Wyoming kimberlites. However, for the Williams diatremes, some colluvial purple, pink, and red garnets that may be from peridotites fill in the gap (fig. 7).

TiO_2 content of Williams garnets is up to 1.1 percent, and the higher TiO_2 garnets are in dunites and harzburgites. Clinopyroxene, the usual host for Ti, is not present or is in very small amounts because of bulk composition, and so the available Ti is in garnet and in spinel.

Analyses of the six color groups (purple, pink, red, red-orange, orange and light orange) of colluvial garnets from the Williams 1 and 4 diatremes (Hearn and McGee, 1982) show that 20 of 21 purple garnets contain more than 2.4 percent Cr_2O_3, which is more than any of the red-orange, orange or light-orange garnets, and 16 purple garnets contain more Cr_2O_3 than any red or pink garnets (fig. 7). Ca-Mg-Fe contents of Mg-rich purple, pink and red colluvial garnets correspond closely to the Ca-Mg-Fe range of peridotite garnets (fig. 6) indicating their probable peridotitic derivation. Many of the Mg-rich red-orange, orange, and light-orange colluvial garnets are similar in Ca-Mg-Fe composition to garnet megacrysts and to peridotitic and pyroxenitic garnets that have lower Cr_2O_3 and CaO contents. The more Fe-rich part of the Ca-Mg-Fe trend suggests that some red-orange, orange and light-orange colluvial garnets are fragments of megacrysts and may extend the megacryst trend to higher Fe contents (fig. 6).

A group of one purple, one light orange and four red Mg-rich colluvial garnets is distinctive in having less than 1 percent Cr_2O_3, 1.0 to 2.9 percent TiO_2 (higher than any red garnets of higher Cr_2O_3 content), and variable Ca for nearly constant Mg/Fe. These garnets may fit group 2 of Dawson and Stephens (1975, 1976)(high-titanium pyrope, all examples are megacrysts or xenocrysts in kimberlite), or may fit groups 25 or 50 of Danchin and Wyatt (1979) that contain some garnets derived from ilmenite-bearing inclusions.

None of the analysed colluvial garnets have the high Cr_2O_3 and low CaO contents that can indicate diamond potential. The Williams kimberlites also lack garnets of high Cr_2O_3-high CaO content (group 12, knorringitic uvarovite-pyrope, Dawson and Stephens, 1975, 1976) that occur sparsely in diamondiferous kimberlites (occurrences summarized in Clarke and Carswell, 1977).

Clinopyroxene

Clinopyroxenes (table 3) range in Mg/(Mg + Fe) from 0.85 for a garnet harzburgite containing phlogopite-ilmenite veins of probable metasomatic origin, to 0.96 for a low-T garnet lherzolite (fig. 8). Clinopyroxenes of highest TiO_2 contents are from the veined harzburgite, from another harzburgite of very low (less than 0.1 percent) clinopyroxene content, and from garnet orthopyroxenite. Na increases in general with increasing Cr (fig. 9). For seven high-T and two low-T inclusions, a systematic relationship of Na and Cr suggests a constant ratio of 0.38 NaCr (ureyite) component to 0.62 NaAl (jadeite) plus Na-ferric Fe (acmite) components. Acmite component calculated by the method of Smyth (1980) is generally very low, less than five percent, and is sensitive to small variations of Si and Al in microprobe analytical data. Clinopyroxenes within garnet clots in low-T lherzolites have Cr_2O_3 contents ranging from 2.2 to 3.4 percent, Al_2O_3 from 2.9 to 4.0 percent, and Na_2O from 2.3 to 3.2 percent.

Orthopyroxene

CaO contents of orthopyroxenes (table 4) generally increase with decreasing Ca/(Ca + Mg) of co-existing clinopyroxene, and are consistent with potential use as a geothermometer (Boyd and Nixon, 1973). Al_2O_3 contents are as high as 1.8 percent, in orthopyroxene from a harzburgite with the highest calculated temperature (H67-28K-3, Hearn and Boyd, 1975). Cr_2O_3 contents of large orthopyroxenes range from 0.1 to 1.1 percent, with the latter value in garnet-spinel lherzolite that contains high-Cr garnet. A small orthopyroxene in a garnet clot (T3-5) contains higher Cr_2O_3, 1.24 percent, due to its local Cr-rich environment.

Olivine

In most inclusions, the forsterite (Fo) content (Mg/(Mg + Fe)) is the same in large strained olivines, small anhedral olivines, and euhedral olivine neoblasts. The harzburgite with phlogopite-ilmenite veins has olivine with the lowest Fo content, 0.83, (table 5, fig. 8), which may indicate an initial cumulate origin, the effects of subsequent equilibration with vein material, or both. Olivine in other peridotites is Fo 89 to 93, with low T-P lherzolites having Fo 91 to 93, high T-P lherzolites having Fo 90 to 93, and olivines from the other harzburgites having Fo 89 to 92. Both garnet dunites contain olivines with Fo between 89 and 90, less than most harzburgites and all of the lherzolites, indicating that the dunites are not refractory residues in relation to the other peridotites of the high T-P group. Similar relative Fo content in dunites compared to lherzolites and harzburgites in kimberlites has been noted by Boyd and Nixon (1973) and others.

Spinel

Analysed spinels from garnet-spinel peridotites (table 6) are all Cr-rich and all are close to the base of the spinel composition prism, within the general kimberlite xenolith trend (Haggerty, 1979). Analysed spinels are from two garnet-spinel dunites and from three low T-P lherzolites which contain abundant small spinels in garnet clots and larger spinels sparsely scattered in the matrix. Spinels observed in garnet-spinel harzburgites have not yet been analysed. Spinels in garnet-spinel dunites and matrix spinels that are distant from garnet clots in lherzolites have similar Cr/(Cr + Al) and Mg/(Mg + Fe) ratios. Spinels in garnet clots are more Mg-rich and Al-rich than matrix spinels (fig. 10). The Montana peridotite spinels are similar to, but slightly less Mg-rich than Lesotho and South African peridotite spinels, and are significantly lower in Mg than those included in diamond (fig. 10).

TiO_2 is highest (3.65-4.06 percent) in spinels of garnet dunite xenoliths, perhaps as a result of being the preferred host for Ti, although the compositions of the garnets (fig. 7) suggest that the assemblage equilibrated with two pyroxenes which can also contain Ti. The occurrences of Cr-rich spinels in Montana garnet peridotites show that Cr-rich spinel and garnet can co-exist over a wide range of T-P conditions.

Phlogopite

Phlogopite has not yet been analysed. It occurs as wide rims around garnets and in the matrix in low T-P lherzolites; and is present in some high T-P peridotites as thin rims around garnet, and in small multi-mineralic inclusions or embayments in garnet. Occurrence of phlogopite in high T-P peridotites contrasts with the observed lack of phlogopite in peridotites of T greater than 1200 degrees C from Lesotho and South Africa (Boyd and Nixon, 1975) but these small amounts of phlogopite may be explained by late metasomatism during kimberlite ascent.

Thermometry and barometry of inclusions

Temperatures (T) in degrees celsius and pressures (P) in kb of equilibration of garnet peridotites and pyroxenite have been calculated by the TEMPEST program of A. A. Finnerty (written communication, 1979). The Williams inclusions are clustered into a high T-P group and a more diffuse low T-P group (fig. 11). The high T-P group has a similar P range and a higher range of T compared to Colorado-Wyoming garnet peridotites. The diffuse low T-P group is between the T-P ranges of garnet peridotites and garnet websterites from Colorado-Wyoming kimberlites (fig. 11). Finnerty and Boyd (1979) found that, for garnet-bearing peridotite and pyroxenite inclusions, the Lindsley-Dixon (1976) 20 kb clinopyroxene solvus for T (with the assumption that pressures greater than 20 kb have negligible effect on the pyroxene solvus) and the MacGregor (1974) method using alumina in orthopyroxene for P gave the best agreement with other observations such as presence of diamond, graphite, or phlogopite. We have used those T-P methods for lherzolite assemblages.

For garnet harzburgites that lack clinopyroxene, we have calculated T by the O'Neill and Wood (1979) olivine-garnet thermometer based on distribution of Fe/Mg, and have calculated pressure by the MacGregor (1974) method. For two garnet dunites, calculated temperatures (1230-1290°C) by the O'Neill-Wood method, for an assumed P of 50 kb, indicate equilibration under conditions similar to those for the high T-P cluster of garnet lherzolites and harzburgites. Slightly higher P (about 53 kb) would place the dunites in the center of the lherzolite-harzburgite cluster, and lower assumed P would place the dunites in a less likely position away from the high T-P cluster. For lherzolites and harzburgites of the high T-P group, the O'Neill-Wood method gives a range of 275 degrees, more than twice the 120 degree range by the Lindsley-Dixon method (fig. 12). The larger range by the O'Neill-Wood method is indicative of the larger effect of small analytical differences in Fe and Mg, slower equilibration of garnet-olivine pairs in comparison to pyroxene pairs, and variable composition of garnets. In addition, the main cluster of O'Neill-Wood temperatures is about 80 to 100 degrees higher than Lindsley-Dixon temperatures (fig. 12), so comparable garnet dunite temperatures could be about 100 degrees lower than plotted on fig. 11.

For two altered lherzolites in which only garnet and clinopyroxene have survived, T has been calculated by the Lindsley-Dixon 20 kb method and P has been calculated by the Mercier (1980) clinopyroxene method for the garnet facies. The comparability of the Mercier (1980) and MacGregor (1974) pressure methods can be tested with fresh lherzolites from Williams diatremes. Calculated Mercier (1980) clinopyroxene pressures range from 10 kb lower to 12 kb higher than MacGregor (1974) pressures. Regardless of that uncertainty, one altered lherzolite is similar in T and P to the low T-P group and the other is similar to the high T-P group.

The high T-P group of lherzolites, harzburgites and dunites lies well above the continental geotherm and within the diamond stability field or on its boundary (fig. 11). The high T-P group is clearly separate from the five lherzolites that lie close to the geotherm at lower T and P. Calculation of T and P by most other methods yields two groups, with a high T-P group generally above the continental geotherm. This pattern, with xenoliths recording higher than normal T in the mantle before their incorporation in the kimberlite, is similar to the T-P distribution of peridotites from other kimberlites in Lesotho, South Africa, and Somerset Island, Canada (Boyd and Nixon, 1975; Mitchell, 1978).

The low T-P inclusions all have coarse texture, whereas both coarse and porphyroclastic textures are represented in the high T-P group. The latter is in contrast to the previous study of only six samples (Hearn and Boyd, 1975), which found only porphyroclastic textures in four high T-P inclusions. Phlogopite is present in larger amounts in low T-P inclusions, and occurs in six of fourteen high T-P inclusions as a minor phase rimming garnet. Phlogopite is unexpected in the high T-P inclusions equilibrated above the kimberlite solidus because the solidus is the approximate limit of phlogopite stability (Eggler and Wendlandt, 1979). Phlogopite may have been metasomatically introduced by the kimberlite host at depth.

For the low T-P garnet-clot lherzolites, the lack of complete equilibrium is reflected by T-P differences for paired pyroxenes that are several mm from clots, close to clots, or within the clots. Large pyroxene grains that are distant from clots are most likely to have retained pre-clot compositions, and give higher calculated P and T. The lowest pressure (fig. 11) is for a pyroxene pair within a clot. Lines connecting separate T-P points tend to parallel the geotherm (fig. 11), and suggest partial re-equilibration toward the spinel-only stability field but remaining within the field of stability of both garnet and spinel. The high-pressure limits of stability of co-existing garnet and spinel are not well defined. MacGregor (1970) found that in the $MgO-CaO-Al_2O_3-SiO_2$ system, as the proportion of Cr_2O_3 to total trivalent oxides increases, the minimum pressure of garnet stability shifts to higher values, and a field of co-existing Cr-rich spinel (chromite) and garnet expands to a wider pressure range. Perkins, Holland and Newton (1981) supported the presence of a widening stability range of spinel plus garnet as Cr content increases, and noted that the co-existence of garnet plus spinel in a single inclusion does not fix temperature and pressure on a single univariant line of garnet-spinel transition. O'Neill's (1981) experiments on lherzolite compositions also showed that increasing Cr raised the pressures for first appearance of garnet and produced a field of coexisting spinel and garnet. The experiments demonstrated that Cr content of spinel co-existing with garnet, two pyroxenes, and olivine can be used to determine pressure. However, O'Neill's results do not define upper limits of spinel stability in the presence of garnet. In natural lherzolitic assemblages, equilibrium of garnet and Cr-spinel persists up to at least 1100 degrees and about 50 kb (Boyd and Nixon 1975; MacGregor, 1979). In dunites and harzburgites, garnet and Cr-spinel co-exist to at least 1150 degrees and 53 kb (Boyd and Finnerty, 1980). In the present study, even higher temperatures (1240-1290 degrees) are calculated for a garnet-spinel dunite (T3-3) by the O'Neill-Wood method for an assumed pressure of 50 kb. For that dunite, calculated pressure is 40.5 kb by the O'Neill (1981) method. However, that pressure seems too low, as it would isolate the dunite from the rest of the high T-P peridotites (fig. 11). Low calculated pressure may be due to lack of equilibrium of garnet and spinel (which both have variable Cr contents), and is less likely to be due to lack of clinopyroxene and orthopyroxene (required for validity of the O'Neill (1981) method), as the lherzolitic $CaO\text{-}Cr_2O_3$ composition of the garnet (fig. 7) implies equilibration with both pyroxenes.

Conclusions

Purple, pink and red colluvial garnets are dominantly Mg- and Cr-rich, indicative of derivation from garnet peridotites or from megacrysts, and are useful for prospecting for kimberlites. Cr-rich, Ca-poor garnets, typical of inclusions in diamond and of diamond-bearing harzburgites from kimberlites elsewhere, are not present in peridotite xenoliths or in the colluvial suite from the Williams kimberlites.

High T-P xenoliths of garnet lherzolite, harzburgite, and dunite of both sheared and granular textures were derived from a part of the upper mantle that is hotter than the typical continental shield geotherm. Textures of the high T-P xenoliths show that deformation was occurring shortly before incorporation in the kimberlite, and for several xenoliths, was followed by static recrystallization under dry or very low water pressure conditions just prior to or during residence in the host kimberlite. In some low T-P garnet-spinel lherzolites, phlogopite-rimmed garnet clots show a disequilibrium texture of partial reaction of higher-Cr garnet to lower-Cr garnet plus clinopyroxene, Cr-spinel, and orthopyroxene prior to inclusion in kimberlite, and later, peripheral partial replacement of garnet by metasomatic introduction of phlogopite. T-P distribution and textures suggest that kimberlitic magma originated deeper than 180 km in a mantle diapir or local mantle thermal anomaly. Kimberlitic magma ascended rapidly (40-70 km/hr) through a heterogeneous high T-P zone (160-190 km depth, within or bordering the diamond stability field) that contained garnet lherzolites, harzburgites and dunites which were being actively deformed on a local scale. In a more shallow zone (100-140km), the kimberlitic magma picked up low T-P peridotites that had partially re-equilibrated in an earlier mantle upwelling event, perhaps related to earlier Paleocene or Eocene magmatism.

Acknowledgements

The authors thank Fred Barnard and personnel of the Anaconda Company for access to claims, sharing of samples, and stimulating discussions in the field. We are deeply grateful to W. E. Williams and Cleo Phillips for access to the area and for gracious hospitality during the study. We are indebted to the late E. L. Williams for pointing out a small outcrop of dark igneous rock to B. C. Hearn, Jr., in 1967, the first clue to the existence of the Williams 1 diatreme. We thank C. P. Sabine, J. J. Papike, N. L. Hickling, H. R. Shaw, J. M. Garihan, F. H. Fowler, H. T. Southworth, K. R. Taylor, C. M. Sears, and W. L. Hearn for assistance in mapping and sampling. We thank F. R. Boyd for providing the initial microprobe analyses, and thank A. A. Finnerty for providing a copy of his TEMPEST program for computing temperatures and pressures of upper mantle inclusions.

References

Boyd, F. R., and Finnerty, A. A., 1980, Conditions of origin of natural diamonds of peridotite affinity: Journal of Geophysical Research, v. 85, p. 6911-6918.

Boyd, F. R., and Nixon, P. H., 1973, Origin of the ilmenite-silicate nodules in kimberlites from Lesotho and South Africa, in Nixon, P. H., ed., Lesotho Kimberlites: Lesotho National Development Corporation, Maseru, p. 254-268.

Boyd, F. R., and Nixon, P. H., 1975, Origins of the ultramafic nodules from some kimberlites of northern Lesotho and the Monastery Mine, South Africa: Physics and Chemistry of the Earth, v. 9, p. 431-454.

Boyd, F. R., and Nixon, P. H., 1978, Ultramafic nodules from Kimberley pipes, South Africa: Geochimica et Cosmochimica Acta, v. 42, p. 1367-1382.

Brockunier, S. R., 1936, Geology of the Little Rocky Mountains, Montana: Unpublished Ph.D. Dissertation, Yale University, 130 p.

Buie, B. F., 1941, Igneous rocks of the Highwood Mountains, Montana. Part III. Dikes and related intrusives: Geological Society of America Bulletin, v. 52, p. 1753-1808.

Bundy, F. P., Bovenkerk, H. P., Strong, H. M., and Wentorf, R. H., 1961, Diamond-graphite equilibrium line from growth and graphitization of diamond: Journal of Physical Chemistry, v. 35, p. 383-391.

Clark, S. P., and Ringwood, A. E., 1964, Density distribution and constitution of the mantle: Reviews of Geophysics, v. 2, p. 35-38.

Clarke, D. B., and Carswell, D. A., 1977, Green garnets from the Newlands kimberlite, Cape Province, South Africa: Earth and Planetary Science Letters, v. 34, p. 30-38.

Danchin, R. V., and Boyd, F. R., 1976, Ultramafic nodules from the Premier kimberlite pipe, South Africa: Carnegie Institution of Washington Yearbook 75, p. 531-538.

Danchin, R. V., and Wyatt, B. A., 1979, Statistical cluster analysis of garnets from kimberlites and their xenoliths: Kimberlite Symposium II, Cambridge, July 1979, Abstracts Volume, (unpaginated).

Dawson, J. B., 1980, Kimberlites and their xenoliths: New York, Springer-Verlag, 252 p.

Dawson, J. B., and Stephens, W. E., 1975, Statistical classification of garnets from kimberlite and associated xenoliths: Journal of Geology, v. 83, p. 589-607.

Dawson, J. B., and Stephen, W. E., 1976, Statistical classification of garnets from kimberlite and associated xenoliths - addendum: Journal of Geology, v. 84, p. 495-496.

Eggler, D. H., McCallum, M. E., and Smith, C. B., 1979, Megacryst assemblages in kimberlite from northern Colorado and southern Wyoming: Petrology, geothermometry-barometry, and areal distribution: Proceedings Second International Kimberlite Conference, American Geophysical Union, v. 2, p. 213-226.

Eggler, D. H., and Wendlandt, R. F., 1979, Experimental studies on the relationship between kimberlite magmas and partial melting of peridotite: Proceedings Second International Kimberlite Conference, American Geophysical Union, v. 1, p. 330-338.

Finnerty, A. A., and Boyd, F. R., 1979, Comparative geothermobarometry: Kimberlite Symposium II, Cambridge, July 1979, Abstracts Volume, (unpaginated).

Gurney, J. J., and Switzer, G. S., 1973, The discovery of garnets closely related to diamonds in the Finsch pipe, South Africa: Contributions to Mineralogy and Petrology, v. 39, p. 103-116.

Harte, Ben, 1977, Rock nomenclature with particular relation to deformation and recrystallisation textures in olivine-bearing xenoliths: Journal of Geology, v. 85, p. 279-288.

Harte, Ben, Cox, K. G., and Gurney, J. J., 1975, Petrography and geological history of upper mantle xenoliths from the Matsoku kimberlite pipe: Physics and Chemistry of the Earth, v. 9, p. 477-506.

Hearn, B. C., Jr., 1968, Diatremes with kimberlitic affinities in north-central Montana: Science, v. 159, p. 622-625.

_____ 1979, Preliminary map of diatremes and alkalic ultramafic intrusions, Missouri River Breaks and vicinity, north-central Montana: U.S. Geological Survey Open-file Report 79-1128, scale 1:125,000.

Hearn, B. C., Jr., and Boyd, F. R., 1975, Garnet peridotite xenoliths in a Montana, U.S.A. kimberlite: Physics and Chemistry of the Earth, v. 9, p. 247-255.

Hearn, B. C., Jr., and McGee, E. S., 1982, Garnets in Montana diatremes: a key to prospecting for kimberlites. U. S. Geological Survey Open-File Report 82-722, 46 p.

Kennedy, C., and Kennedy, G. C., 1976, The equilibrium boundary between graphite and diamond: Journal of Geophysical Research, v. 81, p. 2467-2470.

Knechtel, M. M., 1959, Stratigraphy of the Little Rocky Mountains and encircling foothills, Montana: U. S. Geological Survey Bulletin 1072-N, p. 723-752.

Leighton, V. L., and McCallum, M. E., 1979, Rapid evaluation of heavy minerals in stream sediments of the Prairie Divide area of northern Colorado: a tool for kimberlite exploration: U. S. Geological Survey Open-file Report 79-761, scale 1:24,000.

Lindsley, D. H., and Dixon, S. A., 1976. Diopside-enstatite equilibria at 850° to 1400°C, 5 to 35 kb: American Journal of Science, v. 276, p. 1285-1301.

MacGregor, I. D., 1970, The effect of CaO, Cr_2O_3, Fe_2O_3, and Al_2O_3 on the stability of spinel and garnet peridotites: Physics of the Earth and Planetary Interiors, v. 3, p. 372-377.

MacGregor, I. D., 1974, The system $MgO-Al_2O_3-SiO_2$: Solubility of Al_2O_3 in enstatite for spinel and garnet peridotite compositions: American Mineralogist, v. 59, p. 110-119.

MacGregor, I. D., 1979, Mafic and ultramafic xenoliths from the Kao kimberlite pipe: Proceedings Second International Kimberlite Conference, American Geophysical Union, v. 2, p. 156-172.

Marvin, R. F., Hearn, B. C., Jr., Mehnert, H. H., Naeser, C. W., Zartman, R.E., and Lindsey, D. A., 1980, Late Cretaceous-Paleocene-Eocene igneous activity in north-central Montana: Isochron/West, no. 29, p. 5-25.

McCallum, M. E., and Eggler, D. H., 1976, Diamonds in an upper mantle peridotite nodule from kimberlite in southern Wyoming: Science, v. 192, p. 253-256.

McCallum, M. E., Eggler, D. H., and Burns, L. K., 1975, Kimberlitic diatremes in northern Colorado and southern Wyoming: Physics and Chemistry of the Earth, v. 9, p. 149-161.

McCamy, K., and Meyer, R. P., 1964, A correlation method of apparent velocity measurement: Journal of Geophysical Research, v. 69, p. 691-699.

Mercier, J.-C. C., 1979, Peridotite xenoliths and the dynamics of kimberlite intrusion: Proceedings Second International Kimberlite Conference, American Geophysical Union, v. 2, p. 197-212.

Mercier, J.-C. C., 1980, Single pyroxene thermobarometry: Tectonophysics, v. 70, p. 1-37.

Meyer, H. O. A., and Boyd, F. R., 1972, Composition and origin of crystalline inclusions in natural diamonds: Geochimica et Cosmochimica Acta, v. 36, p. 1255-1273.

Mitchell, R. H., 1978, Garnet lherzolites from Somerset Island, Canada and aspects of the nature of perturbed geotherms: Contributions to Mineralogy and Petrology, v. 67, p. 341-347.

Mitchell, R. H., 1979, Mineralogy of the Tunraq kimberlite, Somerset Island, N.W.T., Canada: Proceedings Second International Kimberlite Conference, American Geophysical Union, v. 1, p. 161-171.

O'Neill, H. St. C., 1981, The transition between spinel lherzolite and garnet lherzolite, and its use as a geobarometer: Contributions to Mineralogy and Petrology, v. 77, p. 185-194.

O'Neill, H. St. C., and Wood, B. J., 1979, An experimental study of Fe-Mg partitioning between garnet and olivine and its calibration as a geothermometer: Contributions to Mineralogy and Petrology, v. 70, p. 59-70.

Perkins, D., III, Holland, T. J. B., and Newton, R. C., 1981, The Al_2O_3 contents of enstatite in equilibrium with garnet in the system $MgO-Al_2O_3-SiO_2$ at 15-40 kbar and 900°-1600°C: Contributions to Mineralogy and Petrology, v. 78, p. 99-109.

Peterman, Z. E., 1981, Archaean gneisses in the Little Rocky Mountains, Montana: U. S. Geological Survey Professional Paper 1199-A, p. 1-6.

Ross, J. V., Ave Lallemant, H. G., and Carter, N. L., 1980, Stress dependence of recrystallized-grain and subgrain size in olivine: Tectonophysics, v. 70, p. 39-61.

Smith, Douglas, Wilson, C. R., and Ehrenberg, S. N., 1982, Interpretation of zoned minerals in garnet lherzolite nodules from minette, Four Corners region: EOS, Transactions American Geophysical Union, v. 63, p. 463.

Smyth, J. R., 1980, Cation vacancies and the crystal chemistry of breakdown reactions in kimberlitic omphacites: American Mineralogist, v. 65, p. 1185-1191.

Sobolev, N. V., Lavrent'ev, Yu. G., Pokhilenko, N. P., and Usova, L. V., 1973, Chrome-rich garnets from the kimberlites of Yakutia and their parageneses: Contributions to Mineralogy and Petrology, v. 40, p. 39-52.

Wood, B. J., 1977, The influence of Cr_2O_3 on the relationships between spinel-and garnet-peridotites: Proceedings Second International Kimberlite Conference, Abstracts Volume, (unpaginated).

Table 1. Relative abundance of types of peridotite and pyroxenite inclusions, Williams 1 and 4 diatremes

	Number
Garnet lherzolite	39
Garnet-spinel lherzolite	12
Spinel lherzolite	17
Lherzolite	5
Garnet harzburgite	5
Garnet-spinel harzburgite	2
Spinel harzburgite	8
Harzburgite	1
Garnet-spinel dunite	2
Spinel dunite	3
Dunite	2
Garnet pyroxenite	3
Spinel pyroxenite	1
Total	100

Table 2. Garnets[1]

	GSL[2] T3-4-2-1-9	GSL T3-4-5	GSL[2] T3-5-1-5-3	GSL T3-5-2	AGL 67-28 E-16	AGL H73-2M	GL 17D-2 Boyd	GL 6C-1 GF-1	GSL 12E1-1-1	GSL 12E2-1-1	GL 15-2-2-2	GH T3-7-4-1	GH 12C-1-1	GH 14-5-1	GH 15-1-2-1	GSD T3-3-2-1	GSD 12M-1-1
SiO_2	41.57	41.28	41.16	41.50	41.65	42.10	40.99	41.99	42.05	40.54	41.81	42.40	42.24	41.82	42.07	41.35	40.24
Al_2O_3	21.46	20.73	20.45	21.21	19.81	21.44	18.58	18.96	19.46	14.99	19.62	19.53	18.47	19.57	20.20	15.83	16.48
FeO	7.34	7.16	7.50	7.14	6.55	7.11	5.68	6.13	6.42	5.63	6.46	6.82	6.21	6.13	7.75	7.32	7.78
MgO	19.73	19.86	19.14	20.17	20.06	21.59	21.43	20.30	20.04	19.42	20.36	20.92	20.65	21.36	19.24	18.73	18.82
CaO	5.96	5.90	5.75	5.29	5.86	4.80	5.71	6.53	6.03	6.79	5.67	5.14	5.30	4.97	5.43	6.58	6.19
TiO_2	.04	05	.01	.04	.00	.60	.50	.23	.09	.75	.36	.67	00	.70	.12	1.08	.81
MnO	.35	.37	.44	.41	.54	.28	.28	.51	.27	.35	.34	.41	.34	.00	.44	.37	.35
Cr_2O_3	4.41	4.55	5.10	3.88	6.08	1.99	6.22	6.43	6.25	10.74	5.41	5.11	6.04	4.97	4.51	9.39	8.14
	100.86	99.90	99.55	99.64	100.55	99.91	99.44	101.08	100.61	99.21	100.03	101.00	99.25	99.52	99.76	100.65	98.81
Si	2.958	2.967	2.977	2.977	2 981	2.991	2.962	2 994	3.003	2.990	2.997	3.008	3.049	2.996	3.027	3.010	2.981
Al	1.801	1.756	1.744	1.795	1.672	1.796	1 583	1 594	1.638	1.303	1.657	1.632	1.571	1.652	1.713	1.358	1.439
Fe	.437	.430	.454	.428	.392	.422	.343	.366	.383	.347	.387	.404	.374	.367	.466	.445	.481
Mg	2.093	2.128	2.064	2.158	2.140	2.287	2.309	2.158	2.134	2.135	2.176	2.212	2.221	2.281	2.064	2.032	2.078
Ca	.454	.454	.446	.407	.449	.365	.442	.499	.461	.536	435	.390	.409	.381	.418	.512	.491
Ti	.002	.002	.000	.002	.000	.032	.027	.012	.005	.041	.019	.035	.000	.037	.006	.059	.044
Mn	.021	.022	.027	024	.033	.017	.017	031	.016	.021	.020	.024	.021	.000	.027	.022	.021
Cr	.248	.258	.292	.220	.344	.112	.355	.362	.352	.626	.306	.286	.344	.281	.256	.540	.476
	8.014	8.017	8.004	8.011	8.011	8.022	8.038	8.016	7.992	7.999	7.997	7.991	7.989	7.995	7.977	7.978	8.011

GSL= garnet spinel lherzolite, AGL= altered garnet lherzolite, GL= garnet lherzolite, GH= garnet harzburgite, GSD= garnet spinel dunite

[1] Analyses in Tables 2-6 were done using an ARL-EMX electron microprobe operating at 15 KV with a 1 micron beam. Standards were natural or synthetic minerals. Analyses are averages of at least two points, and generally three or more points per grain, except as noted. FeO is total Fe as FeO, except for analyses of spinels.

[2] Single analysis

Table 3. Clinopyroxenes

	GSL T3-4-1-1	GSL T3-4-6-2	GSL T3-5-2-5	GSL T3-5-3-1	GSL T3-5-4-2	GSL T3-6-6-2	AGL 67-28-E-16	AGL H73-2M	GL 17D-2 P5-10	GL 6C-1 P3-9	GSL 12E1-4-1	GSL 12E2-3-1	GL 15-2-1-3	GH T3-7-8-3	GH 15-1-1-5
SiO_2	54.06	54.82	55.65	55.94	55.21	55.38	54.10	53.59	53.73	53.79	56.03	55.42	54.50	54.54	55.27
Al_2O_3	2.85	2.78	3.68	2.37	1.88	1.83	2.64	3.23	2.79	2.03	1.26	2.20	1.47	1.23	2.14
FeO	2.32	2.25	2.31	2.05	2.02	2.24	2.04	3.67	2.72	3.15	3.05	2.53	3.14	3.37	5.02
MgO	15.18	15.75	14.70	16.21	16.71	16.72	16.09	19.55	19.32	19.66	21.09	19.61	20.72	19.77	17.08
CaO	18.77	19.85	18.63	20.67	20.55	20.01	19.00	15.52	16.76	17.20	18.61	15.84	17.37	17.31	18.19
Na_2O	2.53	2.23	3.14	2.27	1.86	2.10	2.44	1.68	1.64	1.06	.60	2.01	.93	1.32	2.00
TiO_2	.17	.09	.11	.17	.08	.16	.15	.17	.22	.06	.00	.35	.22	.40	.26
MnO	.07	.12	.00	.00	.00	.12	.20	.00	.13	.00	.04	.00	.00	.00	.19
Cr_2O_3	2.91	1.87	3.07	2.01	1.65	2.25	2.22	.71	1.76	1.16	.89	2.88	1.08	2.66	1.13
	98.86	99.76	101.29	101.69	99.96	100.81	98.88	98.12	99.07	98.11	101.57	100.84	99.43	100.60	101.28
Si	1.977	1.983	1.982	1.986	1.992	1.986	1.974	1.954	1.947	1.967	1.978	1.968	1.967	1.958	1.982
Al	.122	.118	.154	.099	.079	.077	.114	.138	.118	.088	.052	.091	.062	.051	.090
Fe	.070	.068	.068	.061	.060	067	.062	.111	.082	.096	.090	074	.094	.101	.150
Mg	.827	.849	.780	.858	.899	.893	.875	1.062	1.044	1.072	1.110	1.038	1.114	1.058	.913
Ca	.735	.769	.710	.786	.794	.769	.742	.606	.650	674	.704	.602	.671	.665	.698
Na	.179	.156	.216	.156	.130	.146	.172	.119	.115	.075	.040	.138	.065	.091	.138
Ti	.004	.002	.002	.004	.002	.004	004	.004	.005	.002	.000	.009	.006	.010	.006
Mn	.002	.003	.000	.000	.000	.003	.005	.000	.004	.000	.001	.000	.000	.000	.005
Cr	.084	.053	.086	.056	.046	.063	.064	.020	.050	.034	.024	.080	.030	.075	.032
	4.000	4.001	3.998	4.006	4.002	4.008	4.012	4.014	4.015	4.008	3.999	4.000	4.009	4.009	4.014

GSL= garnet spinel lherzolite, AGL= altered garnet lherzolite, GL= garnet lherzolite, GH= garnet harzburgite

Table 4. Orthopyroxenes

	GSL T3-4-1-2	GSL T3-4-6-1	GSL T3-5-3-2	GSL T3-5-4-1	GSL T3-5-2-6	GSL T3-6-2-2	GL 17D-2 P5-11	GL 6C-1 P3-10	GSL 12E1-1-2	GSL 12E2-1-2	GL 15-2-3-3	GH T3-7-8-1	GH 12C-1-2	GH 14-7-2	GH 15-1-1-6
SiO_2	57.59	57.97	58.44	58.54	57.54	57.18	56.61	56.19	57.27	57.52	57.17	56.84	57.29	57.31	56.84
Al_2O_3	.72	.82	.87	.67	2.27	.89	1.55	1.41	1.20	1.13	1.31	1.38	1.32	1.57	.61
FeO	4.72	4.71	4.65	4.62	3.88	4.74	4.43	5.08	4.88	4.42	4.90	5.25	4.85	4.58	8.86
MgO	36.00	36.48	36.48	36.96	35.21	36.57	34.54	34.24	35 29	35.35	35.18	34 29	35.72	35.18	33.12
CaO	.41	.28	.33	.31	.99	.24	1.25	1.36	1.37	1.14	1.33	1.25	1.10	1.21	.61
Na_2O	.10	.07	.11	.12	.20	.00	.30	.13	.11	.32	.15	.35	.14	.34	.20
TiO_2	.00	.06	.12	.00	.07	.00	.00	.01	.00	.14	.08	.11	.00	.26	.18
MnO	.00	.16	.09	.15	.16	.12	.09	.10	.09	.10	.23	.00	.00	.05	.17
Cr_2O_3	.31	.33	.35	.29	1.24	.33	.60	.64	.58	1.09	.56	.87	.52	.65	.13
	99.85	100.88	101.44	101.66	101.56	100.07	99.37	99.16	100.79	101.21	100.91	100.34	100.94	101.15	100.72
Si	1.974	1.968	1.971	1.971	1.941	1.958	1.956	1.953	1 955	1.955	1.951	1.954	1.951	1.948	1.971
Al	.029	.032	.034	.026	.090	.035	.063	.058	.048	.045	.052	.055	.053	.063	.024
Fe	.135	.133	.131	.130	.109	.135	.128	.148	.139	.125	.139	.150	.138	.130	.256
Mg	1.840	1.846	1.834	1.855	1.771	1.867	1.779	1.774	1.796	1.790	1.790	1.757	1.813	1.782	1.712
Ca	.014	.010	.012	.011	.035	.008	.046	.051	.049	.041	.048	.046	.040	.043	.022
Na	.006	.004	.006	.007	.012	.000	.019	.009	.007	.021	.009	.023	.009	.022	.013
Ti	.000	.001	.002	.000	.001	000	.000	.000	.000	.004	.002	.002	.000	006	.004
Mn	.000	.004	.002	.004	.004	.003	.002	.003	.002	.003	.006	.000	.000	.001	.004
Cr	.008	.008	.009	.007	.033	.008	.016	.018	.015	.029	.014	.023	.013	.017	.003
	4.006	4.006	4.001	4.011	3.996	4.014	4.009	4.013	4.011	4.013	4.011	4.010	4.017	4.012	4.009

GSL= garnet spinel lherzolite, GL= garnet lherzolite, GH= garnet harzburgite

Table 5. Olivines

	GSL T3-4-1-3	GSL T3-4-6-3	GSL T3-5-5-7	GSL T3-5-8-1	GSL T3-6-6-1	GL 17D-2 P5-13	GL 6C-1 P3-11	GSL 12E1-3-3	GSL 12E2-4-1	GL 15-2-4-3	GH T3-7-4-3	GH 12C-1-3	GH 14-2-3	GH 15-1-6-4	GSO T3-3-2-2	GSD 12M-6-1
SiO_2	40.99	41.20	41.85	41.61	41.01	40.39	40.06	40.60	41.46	42.12	40.44	41.54	41.68	40.75	39.88	40.55
FeO	7.81	9.11	8.05	7.88	8.25	7.48	8.86	8.48	7.31	8.73	9.53	8.00	8.04	15.78	10.11	10.35
MgO	51.51	49.55	49.87	49.45	50.60	50.88	49.47	48.63	51.13	49.23	50.09	49.80	50.62	44.68	49.22	48.05
CaO	.00	.00	.02	.00	.00	.10	.03	.11	.07	.26	.06	.09	.16	.01	.09	.03
TiO_2	.00	.00	.02	.00	.05	.09	.00	.04	.01	.06	.04	.04	.08	.07	.06	.01
MnO	.09	.08	.16	.13	.00	.03	.19	.11	.00	.24	.13	.18	.00	.20	.18	.19
Cr_2O_3	.00	.18	.00	.00	.07	.00	.17	.00	.18	.04	.00	.17	.14	.02	.34	.11
NiO	.42	.38	.37	.41	.35	.32	--	.38	.36	.40	.31	.35	.29	.22	.35	.38
	100.82	100.50	100.34	99.48	100.33	99.29	98.78	98.35	100.52	101.08	100.60	100.17	101.01	101.73	100.23	99.67
Si	.989	1.002	1.012	1.015	.995	.988	.992	1.006	.999	1.015	.986	1.008	1.002	1.008	.980	1.000
Fe	.157	.185	.162	.160	.167	.153	.183	.175	.147	.176	.194	.162	.161	.326	.207	.213
Mg	1.853	1.796	1.799	1.798	1.831	1.856	1.824	1.797	1.838	1.770	1.821	1.801	1.815	1.646	1.805	1.768
Ca	.000	.000	.000	.000	.000	.002	.001	.003	.001	.006	.001	.002	.004	.000	.002	.000
Ti	.000	.000	.000	.000	.000	.001	.000	.000	.000	.001	.000	.000	.001	.001	.001	.000
Mn	.001	.001	.003	.002	.000	.000	.004	.002	.000	.004	.002	.003	.000	.004	.003	.004
Cr	.000	.003	.000	.000	.001	.000	.003	.000	.003	.000	.000	.003	.002	.000	.006	.002
Ni	.008	.007	.007	.007	.006	.006	--	.007	.006	.007	.006	.006	.005	.004	.006	.007
	3.008	2.994	2.983	2.982	3.000	3.009	3.007	2.990	2.994	2.979	3.010	2.985	2.990	2.989	3.010	2.994

GSL= garnet spinel lherzolite, GL= garnet lherzolite, GH= garnet harzburgite, GSD= garnet spinel dunite
--Not analyzed

Table 6. Spinels

	GSL T3-4-5-7	GSL T3-4-9-6	GSL T3-5-1-13	GSL T3-5-9-2	GSL T3-6-1-4	GSD T3-3-3-3	GSD 12M-4-4
SiO_2	.49	.62	.60	.71	.47	.70	.81
Al_2O_3	13.77	9.37	13.37	6.89	5.33	8.49	9.24
Fe_2O_3*	4.21	3.79	3.67	3.90	4.91	4.61	4.72
FeO*	15.67	17.39	16.06	16.78	17.72	17.47	17.77
MgO	12.92	11.63	12.46	11.89	10.86	13.56	13.32
TiO_2	.40	.82	.23	1.30	1.60	4.06	3.65
Cr_2O_3	53.59	57.16	53.89	58.17	57.71	52.64	52.11
NiO	.13	.17	.13	.18	.17	.28	.27
	101.18	100.95	100.41	99.82	98.77	101.81	101.89
Si	.015	.020	.019	.024	.016	.022	.026
Al	.512	.359	.503	.269	.213	.320	.347
Fe3+	.100	.093	.088	.097	.125	.111	.113
Fe2+	.414	.472	.429	.464	.503	.467	.474
Mg	.608	.563	.593	.587	.549	.646	.633
Ti	.010	.020	.005	.032	.041	.098	.088
Cr	1.338	1.468	1.359	1.522	1.548	1.330	1.313
Ni	.003	.004	.003	.005	.005	.007	.007
	3.000	2.999	2.999	3.000	3.000	3.001	3.001

* FeO and Fe_2O_3 values are calculated, cation total normalized to 3.
GSL= garnet spinel lherzolite, GSD= garnet spinel dunite.

Fig. 1

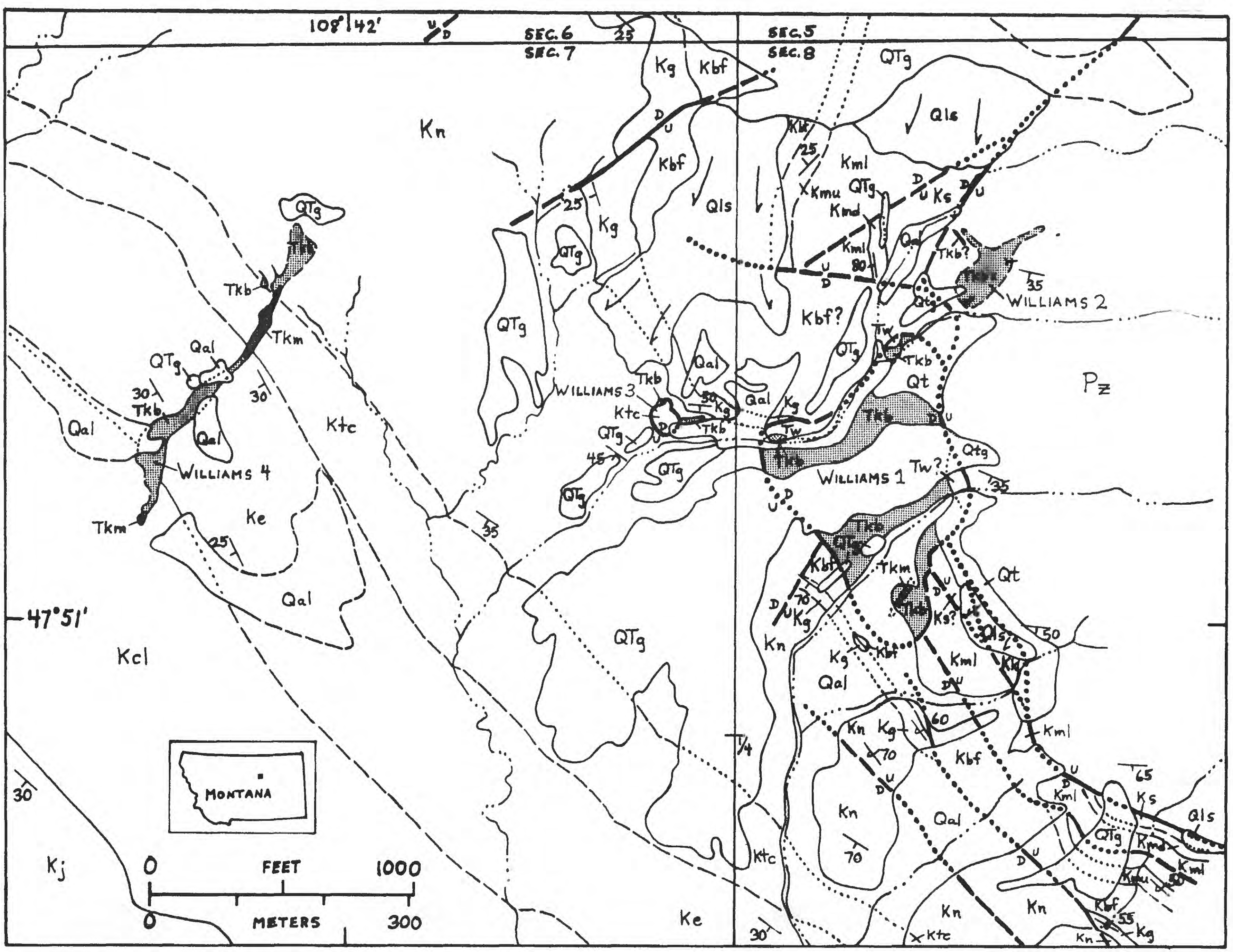

Fig. 1. Geologic map of Williams kimberlite diatremes, north-central Montana, U.S.A.

Figure 1: EXPLANATION

Qal	Qal	Alluvial and colluvial deposits	Holocene and Pleistocene	QUATERNARY
Qls	Qls	Landslide deposits		
Qt	Qt	Talus deposits		
QTg		Terrace and pediment gravel deposits	Pleistocene and Pliocene?	
Tkm Tkb	Tkm Tkb	Massive kimberlite Kimberlite breccia	Middle Eocene	TERTIARY
Tw		Wasatch Formation	Lower Eocene	
Kj		Judith River Formation	Upper Cretaceous	CRETACEOUS
Kcl		Claggett Shale		
Ke		Eagle Sandstone		
Ktc		Telegraph Creek Formation		
Kn		Niobrara Formation and Carlile Shale		
Kg		Greenhorn Formation and Mosby Sandstone Member of Belle Fourche Shale		
Kbf		Belle Fourche Shale		
Kmu		Mowry Shale, upper member	Lower Cretaceous	
Kml		Mowry Shale, lower member		
Kmd		Muddy Sandstone		
Ks		Skull Creek Shale		
Kk		Kootenai Formation		
Pz		Paleozoic, undivided	Lower Miss. to Cambrian	PALEOZOIC


Contact, dashed where approximately located, dotted where concealed

Fault, dashed where approximately located, dotted where concealed; U, upthrown side; D, downthrown side

Strike and dip of inclined, vertical and overturned beds


Prospect pit


Adit


Arrows indicate direction of landslide movement

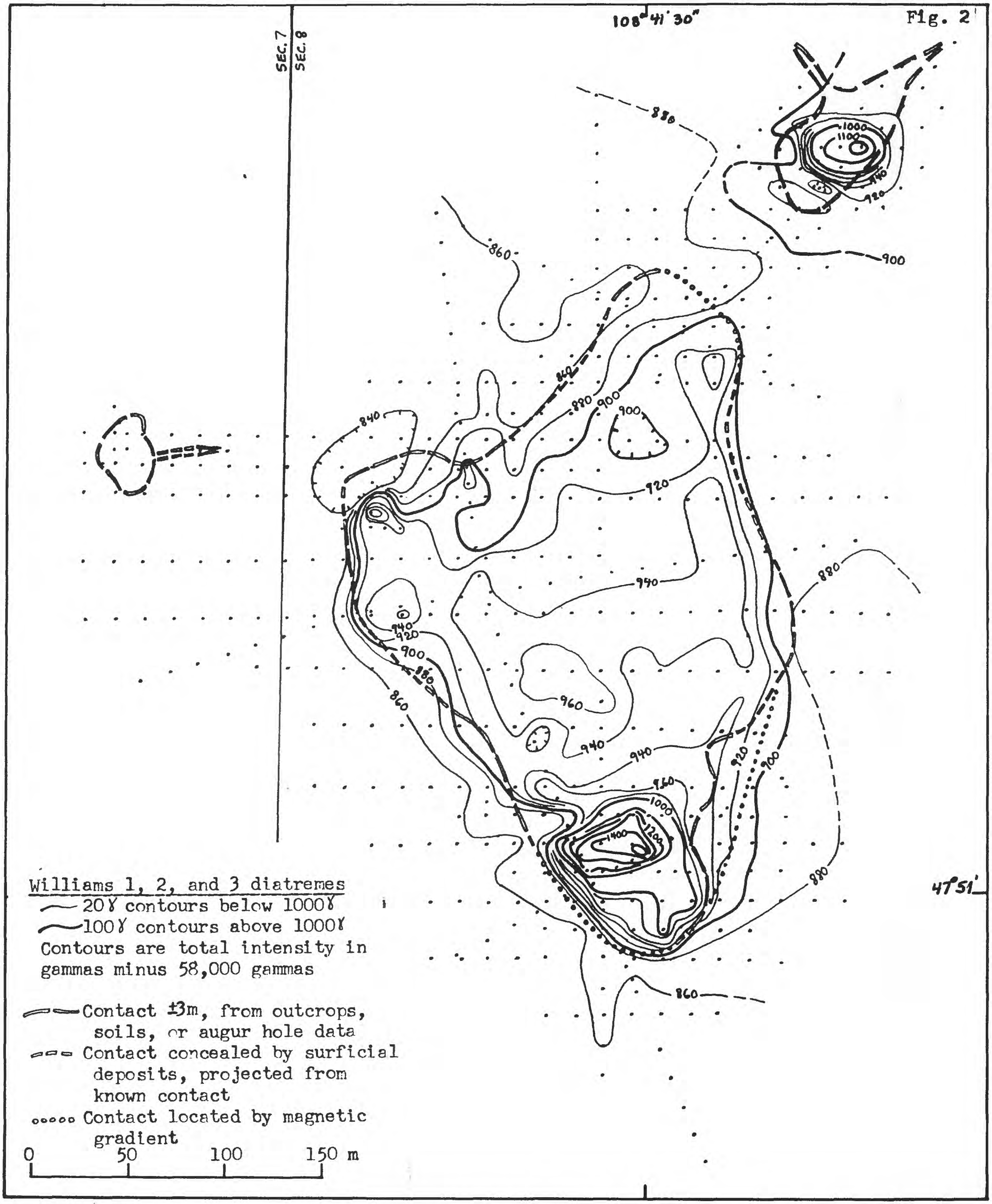

Fig. 2. Magnetic map of Williams 1, 2 and 3 diatremes.

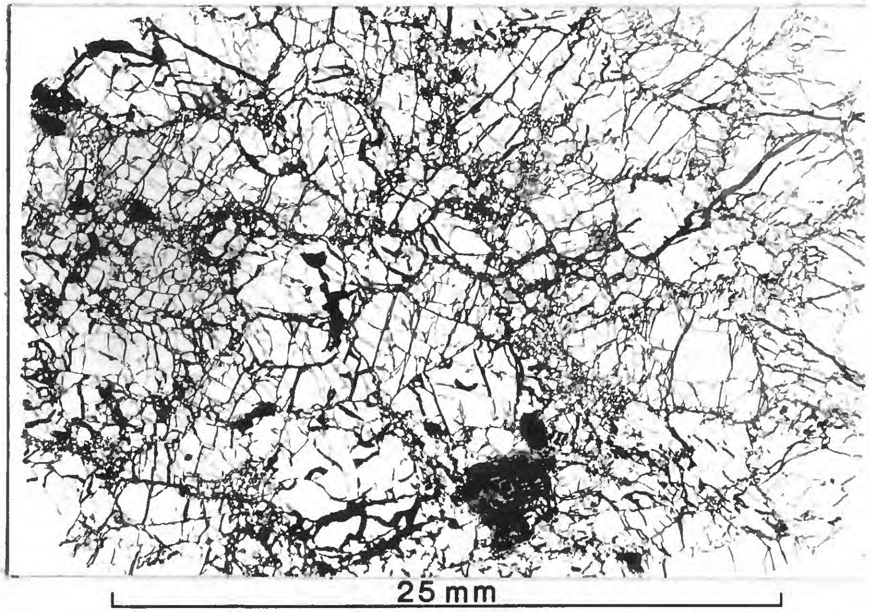

Fig. 3. Photomicrograph of porphyroclastic garnet-spinel dunite T3-3 showing partly altered garnets (dark), large strained olivines with necklace texture of small recrystallized anhedral olivines and sparse euhedral olivine neoblasts; plane light.

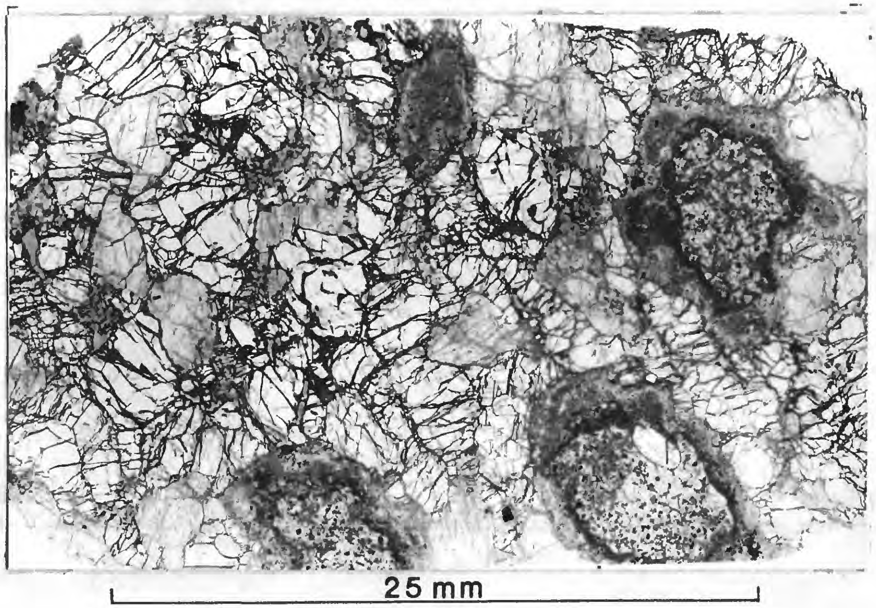

Fig. 4. Photomicrograph of low T garnet lherzolite T3-4 with garnet-clinopyroxene-spinel$\pm$orthopyroxene clots; plane light.

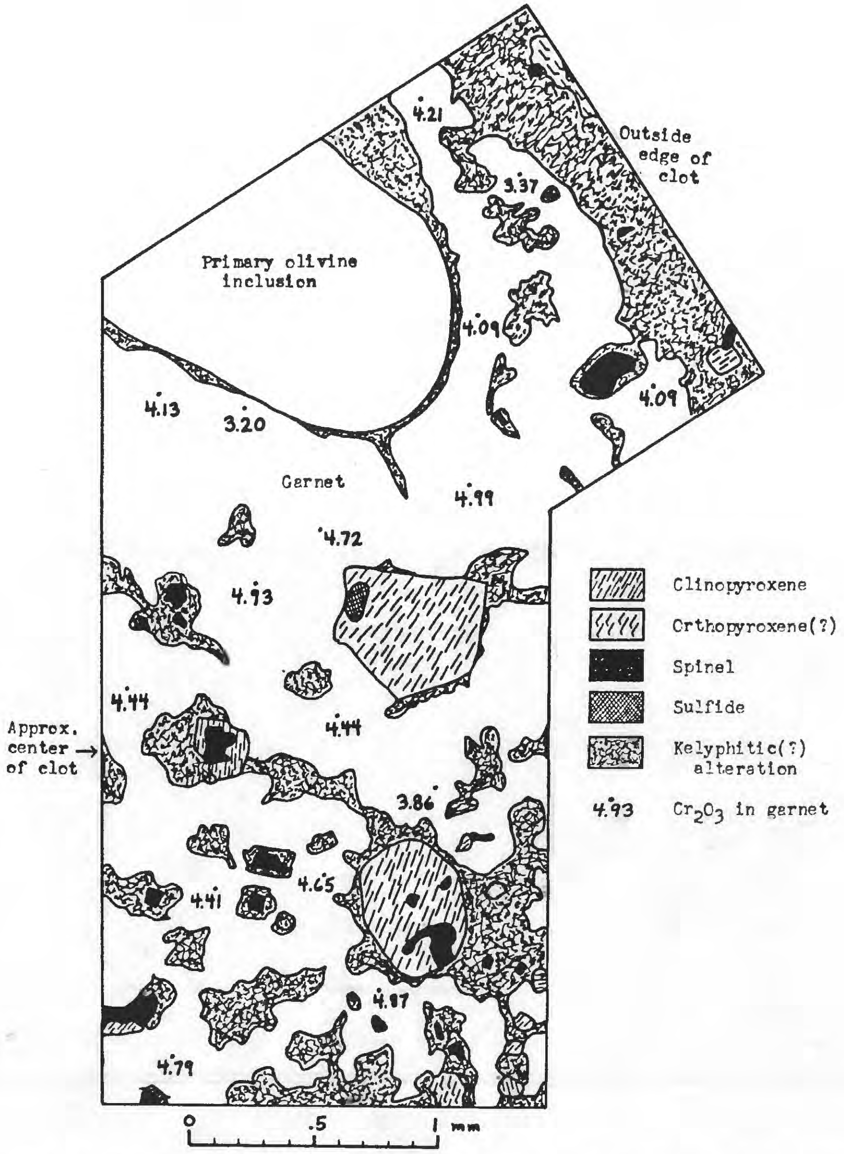

Fig. 5. Detail of garnet clot in T3-4 showing varying Cr_2O_3 content of garnet.

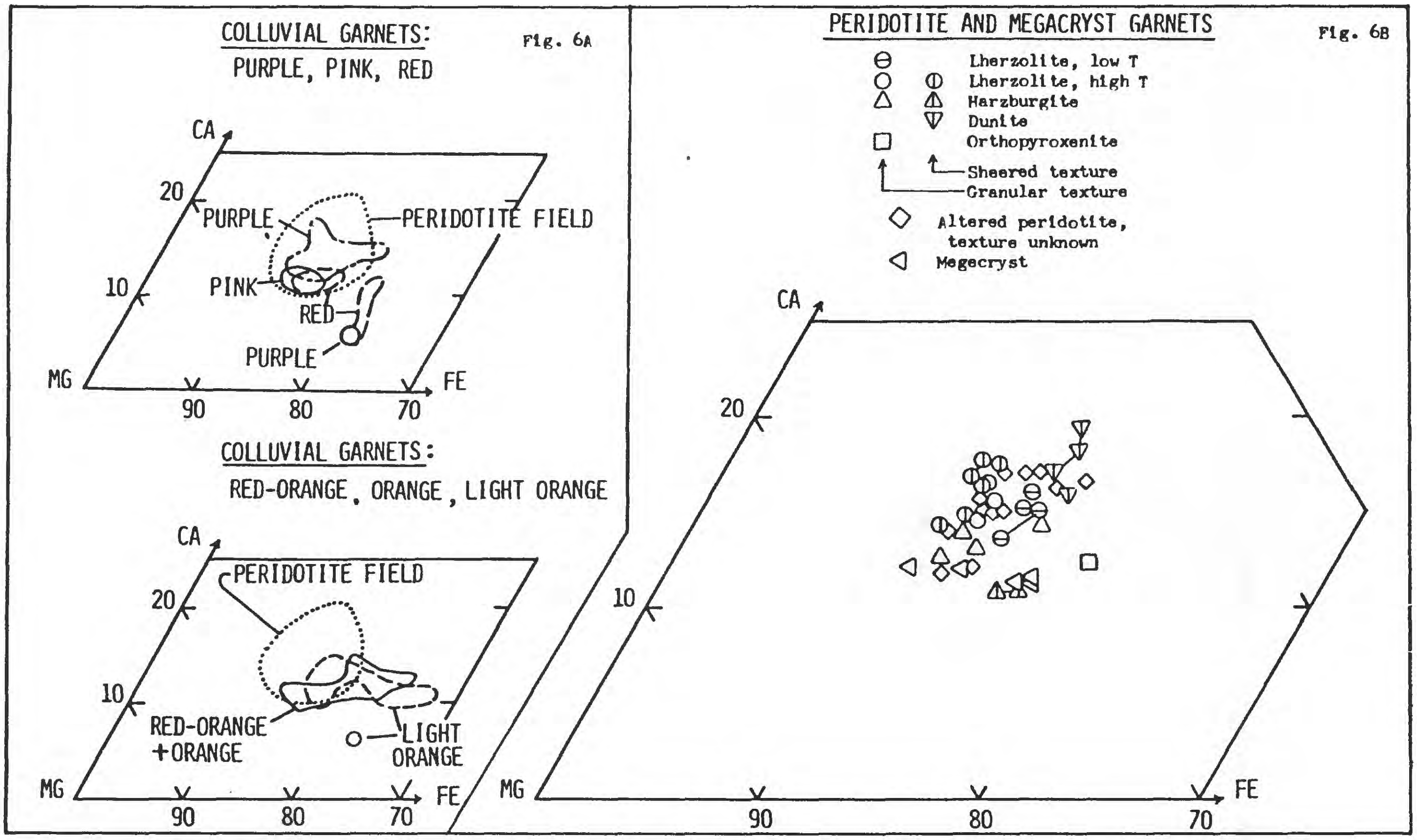

Fig. 6. Ca-Mg-Fe compositions of garnets. A, Mg-rich colluvial garnets classified by color. B, Megacryst, peridotite and pyroxenite garnets.

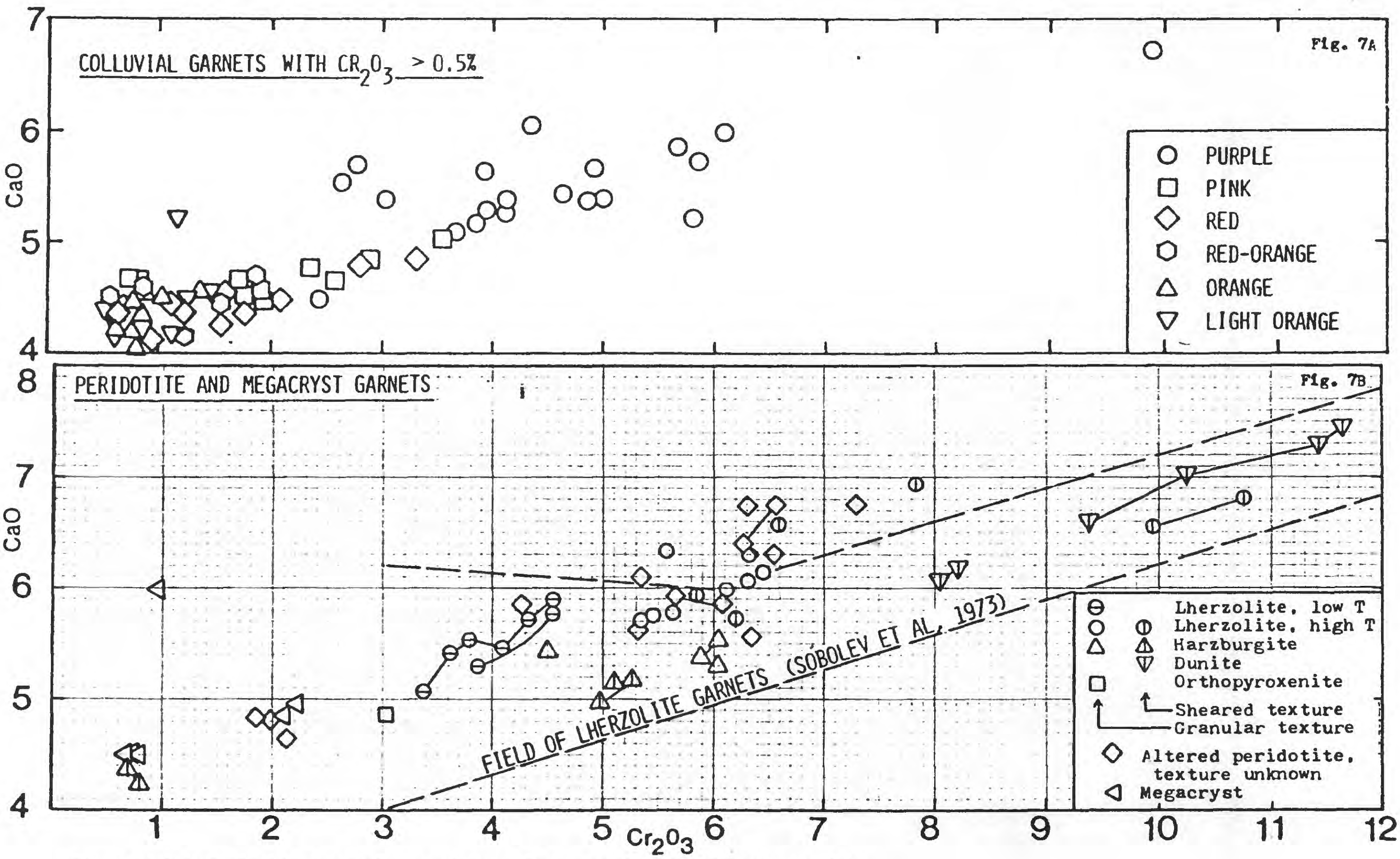

Fig. 7. CaO-Cr_2O_3 (weight percent) compositions of garnets. A, Colluvial garnets with more than 0.5 Cr_2O_3. B, Garnet megacrysts and garnets from peridotites and pyroxenite.

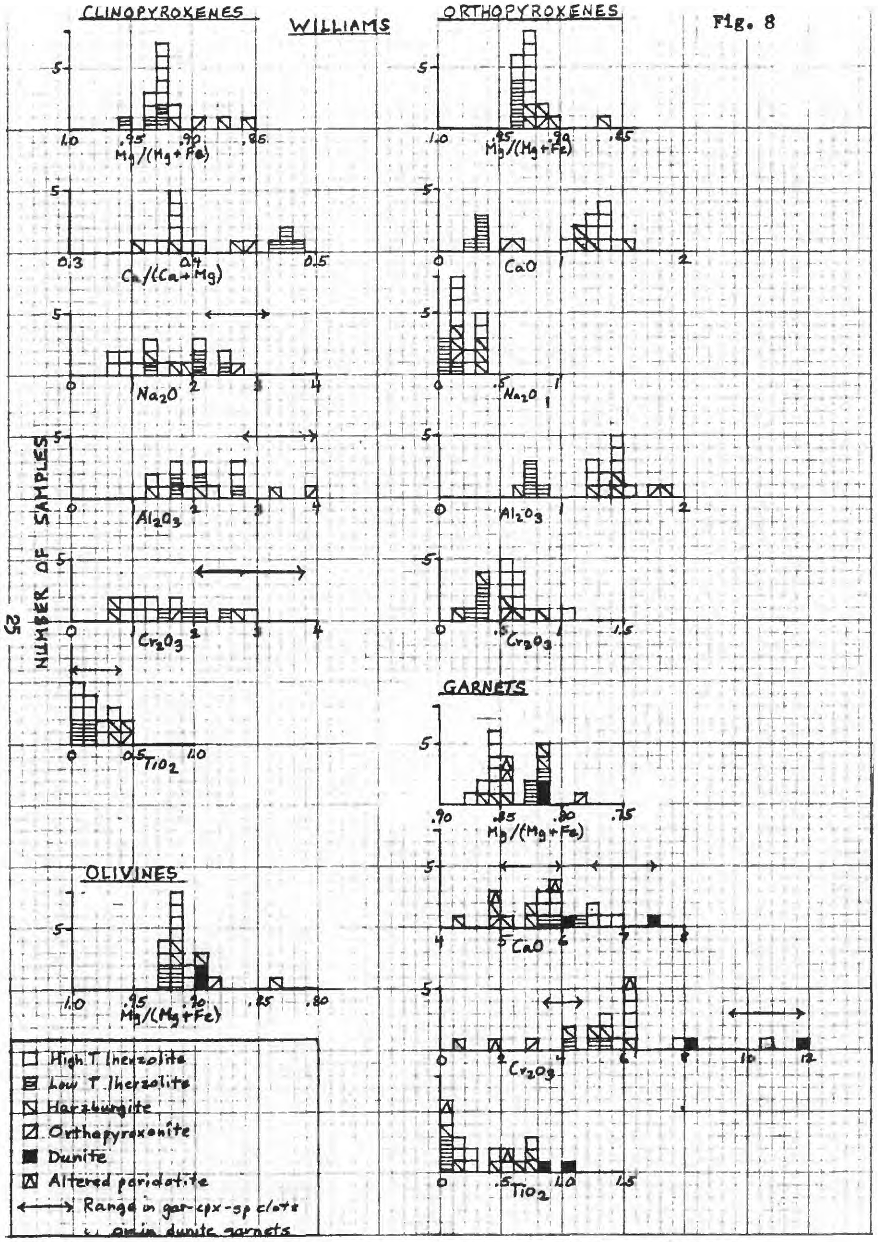

Fig. 8. Histograms of clinopyroxene, orthopyroxene, olivine, and garnet compositions in garnet peridotites and garnet orthopyroxenite, showing range of some oxide compositions in garnet-clinopyroxene-spinel clots in low T garnet lherzolites, and in dunite garnets.

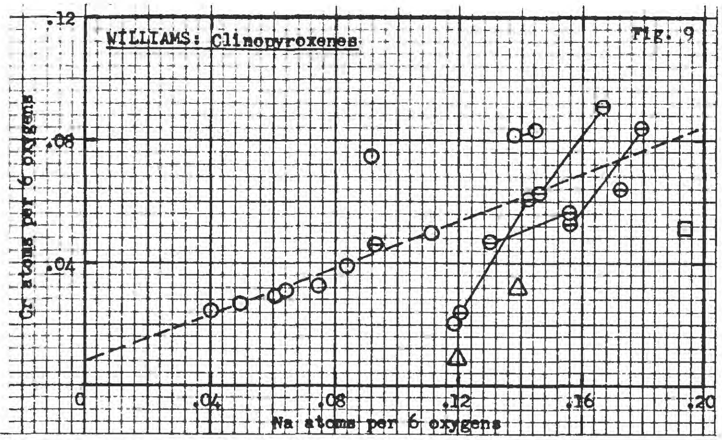

Fig. 9. Cr atoms vs. Na atoms (per 6 oxygens) for clinopyroxenes in garnet lherzolites, garnet harzburgites, and garnet orthopyroxenite; open circle, high T lherzolite; lined circle, low T lherzolite; triangle, harzburgite; square, orthopyroxenite. Solid lines show variation, particularly in low T garnet-clot lherzolites. Dashed line suggests a constant ratio of 0.38 NaCr component to 0.62 NaAl plus NaFe components in clinopyroxenes from seven high T and two low T peridotites.

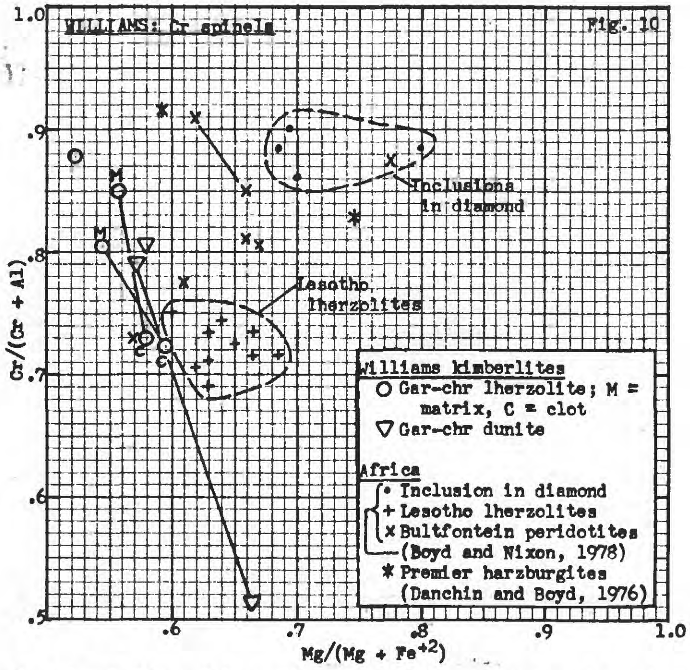

Fig. 10. Cr/(Cr + Al) vs. Mg/(Mg + Fe+2) for chromium-rich spinels in Williams low T garnet-spinel lherzolite and garnet-spinel dunites compared to other chromites. Lines show variation in single inclusions.

Fig. 11

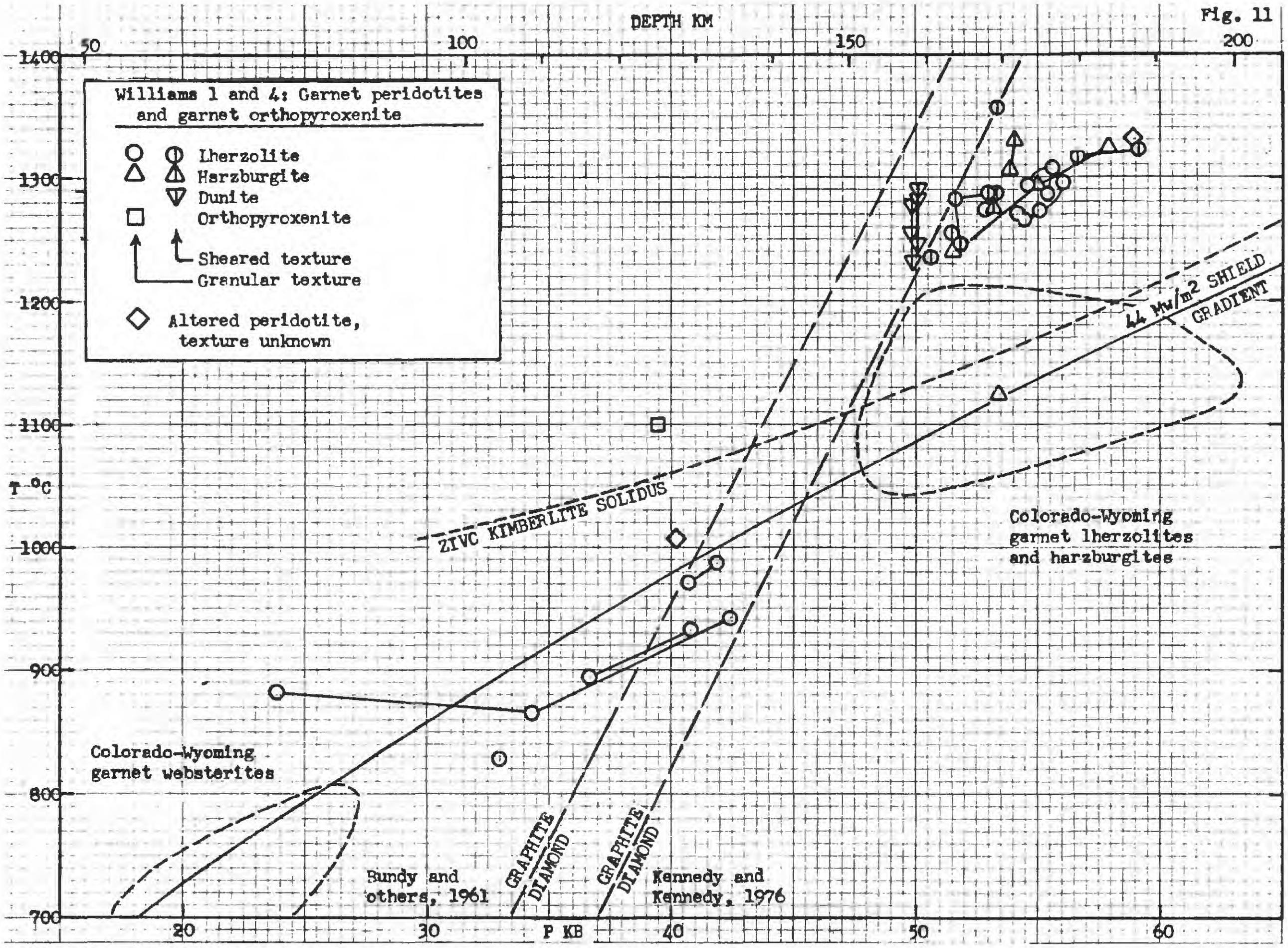

Fig. 11. Calculated temperatures and pressures of garnet peridotites and garnet orthopyroxenite from Williams diatremes, Montana. Diamond-graphite boundaries from Bundy and others (1961) and Kennedy and Kennedy (1976); shield geothermal gradient from Clark and Ringwood (1964); kimberlite solidus and ZIVC (zone of invariant vapor composition, approximate upper limit of phlogopite stability) from Eggler and Wendlandt (1979). P-T fields of Colorado-Wyoming xenoliths from Eggler, McCallum and Smith (1979) based on T from the Lindsley and Dixon (1976) solvus and P by the Wood (1977) method.

Fig. 12

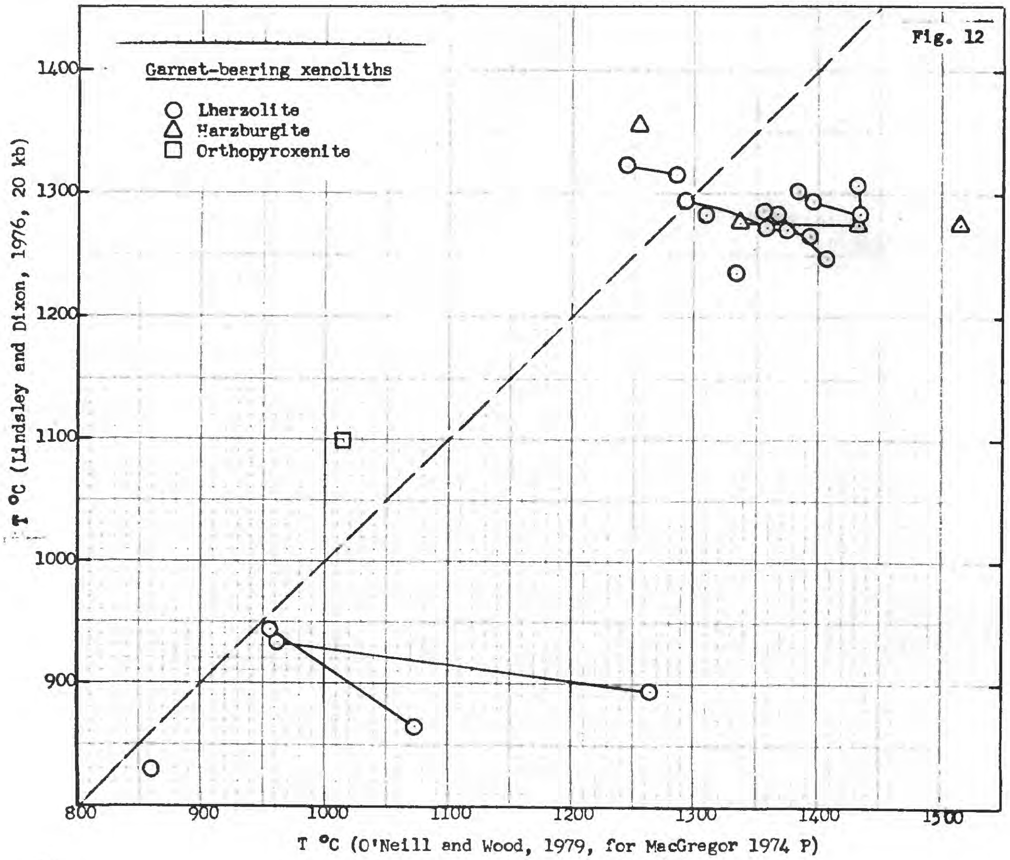

Fig. 12. Comparison of Lindsl and Dixon (1976) 20 kb tempera tures and O'Neill and Wood (1979) temperatures for MacGregor (1974) pressures, for garnet lherzolites, garnet harzburgites containing clino- pyroxene, and garnet pyroxenit